Electrodeposition of zinc–nickel alloy by pulse plating using non-cyanide bath

S. Mohan*, V. Ravindran, B. Subramanian and G. Saravanan

In this study, zinc–nickel electrodeposition was carried out in a sulphamate bath at pH 3–4 by pulse plating and the deposits obtained were characterised by measuring microhardness, surface roughness and by employing SEM, XRD, AFM techniques. The corrosion behaviour of the deposits was evaluated by potentiodynamic polarisation. The deposits obtained by pulse plating have an increased Ni content, thought to be responsible for an improved corrosion resistance.

Keywords: Zn–Ni, Pulse plating, XRD, AFM, Potentiodynamic polarisation

Introduction

In recent times, the most widely used corrosion protective coating for steel has been zinc which is coated on steel either by hot dipping or electroplating. For good corrosion protection, the coating thickness should be 25 μm. Owing to certain disadvantages of thicker coatings, e.g. weldability and formability are poor when thick coatings are used, the current interest is in the development of thin coatings. Alloys of zinc with nickel have five to six times better corrosion resistance than zinc.[1–4] It has been further shown that the formability[5] and weldability[6] of zinc–nickel alloy coated steel are good.

Although zinc–nickel alloy electrodeposits are mainly used as coatings to improve the corrosion resistance of automobile steel bodies, these coatings have been considered for several other applications such as for electrocatalytic water electrolysis,[6,7] coating for steel cord reinforcement of tyres[8] and in the electronics industry.[9] Zinc–nickel alloys have also been considered as alternative coatings to cadmium.[10,11] Since cadmium is a toxic metal leading to health hazards and risk of pollution, environmental regulations are encouraging the use of alternative systems.[12]

Pulse plating has several advantages over conventional plating. Current density, on time, off time and frequency can all be varied. Because of this, pulse plating has received considerable interest over the past 20 years and has proved to be a successful route for materials processing.[13–18] Pulse plating improves deposit properties such as porosity, ductility, hardness and surface roughness. Pulse electrodeposition can be used as a means to produce a unique structure, i.e. coatings with properties not obtained by direct current plating. Pulse electrodeposition also yields a finer grained homogeneous surface appearance of the deposit, because a higher instantaneous current density is possible during deposition. Pulse plating can also yield uniformity in alloy composition and grain structure, smoother and denser deposits with negligible porosity. For alloy codeposition, pulse plating can produce compositions and structures that are not obtainable in dc plating.[19] With pulse current, the average current density can be increased to 8 A dm^{-2}, whereas in direct current, only up to 4 A dm^{-2} can be achieved.[20] Because of this, the percentage of nickel can be increased to 20% in zinc–nickel alloy. Even though a large volume of literature is available on the electrodeposition of zinc–nickel alloys, no systematic work is believed to have been carried out for this using pulse plating.

It is generally accepted that the highest corrosion resistance of zinc–nickel alloys can be obtained with nickel content in the 10–15% range. A search for a non-cyanide zinc plating bath resulted in the development of a zinc–nickel sulphamate bath,[21] yielding grey, uniform and semibright deposits in the presence of boric acid, sodium lauryl sulphate and β-napthol.

Experimental

Surface preparation of substrates

Mild steel having the following composition in wt-%, was used: Fe–0·003C–0·23Mn–0·03S–0·011P.

The Zn–Ni coatings were deposited on mild steel substrates using pulse plating. Coupons of the substrate were cut to an approximate size of 75×25 mm and polished well mechanically using 1/0, 2/0, 3/0 and 4/0 emery papers successively. The polished substrates were degreased with acetone and then cathodically cleaned in alkali solution containing sodium hydroxide and sodium carbonate for 2 min at 70°C, and rinsed with distilled water. Pulse plating of Zn–Ni layers was then carried out on the smooth and clean mild steel panels as described below. pH measurements were made using a TESTRONICS 511 Digital pH meter. The pH of the bath was maintained at 3·5–4, using 5%H$_2$SO$_4$.

Pulse plating of Zn–Ni

Pulse plating was carried out using a DYNATRONIX, model DPR 20-5-10 current generator.

The formulae used for determining various parameters are given below

Central Electrochemical Research Institute, Karaikudi 630 006, India

*Corresponding author, email sanjnamohan@yahoo.com

$$\text{Duty cycle} = \frac{\text{on time} \times 100}{\text{on time} + \text{off time}} \qquad (1)$$

$$\text{Average current} = \frac{\text{on time} \times \text{peak current}}{\text{total time}} \qquad (2)$$

$$\text{Peak current} = \frac{\text{average current}}{\text{duty cycle}} \qquad (3)$$

Table 1 gives the composition of the zinc–nickel bath used for plating and the operating conditions employed. Pulse plating was carried out on an area of one square inch, at room temperature and 40°C, for 30 min, at current densities 0·5 and 1·5 A dm^{-2} under the conditions given in Table 2.

Characterisation

The crystallographic structure of the Zn–Ni alloy coatings were analysed with an X'PERT PRO PHILIPS X-ray diffractometer using Cu K_α line. The microstructure of the coatings was examined using a Hitachi S-3000H scanning electron microscope and a molecular imaging atomic force microscope. Microhardness of the Zn–Ni coated steels was evaluated using a DM 400 microhardness tester from LECO with Vickers indentors. A diamond pyramid was pressed into the deposit under a load of 25 g for 15 s and the indentation diagonal measured after the load was removed. The microhardness in kg mm^{-2} was determined in each case using the formula

$$H_V = 1854 \frac{L}{d^2} \qquad (4)$$

where L is the applied load in g and d is the diagonal of the indentation in μm.

The composition of the coatings was analysed on a HORIBA X-ray analytical microscope XGT 2000 employing the X-ray fluorescence technique. The surface roughness of the coating was measured using a MITUTYO profilometer. The corrosion resistance of the deposit was assessed by electrochemical polarisation studies using an AUTOLAB PG Stat 30.

Molecular imaging was carried out with a SiN tip, contact mode; 5×5 μm scanned area. Corrosion resistance measurements were performed using a three electrode assembly. The samples were masked with lacquer to expose an area of 1 cm^2 on one side of the working electrode. A large platinum foil (6·25 cm^2) and saturated calomel electrode were employed as auxiliary and reference electrodes respectively. Polarisation studies were carried out in 3·5 wt-% neutral sodium chloride solutions at room temperature (28°C). The working electrode was introduced into the test solution and it was allowed to attain a steady state potential

Table 1 Standard bath compositions and operating conditions of sulphamate Zn–Ni plating bath

Zinc sulphamate, M	0·5
Nickel sulphamate, M	0·5
Boric acid, M	0·84
NH$_4$Cl, M	1·12
β-naphthol, M	0·865
Sodium lauryl sulphate, M	0·865
pH	3–4
Temperature, K	328
Stirring	Yes
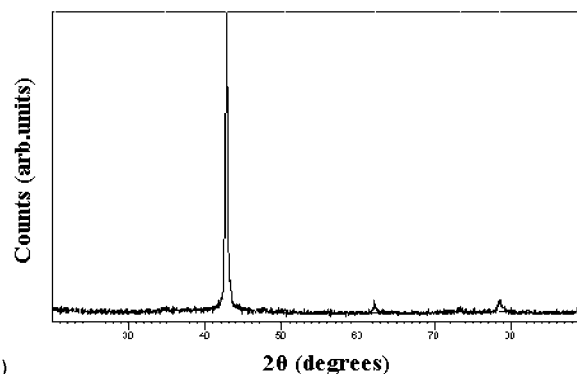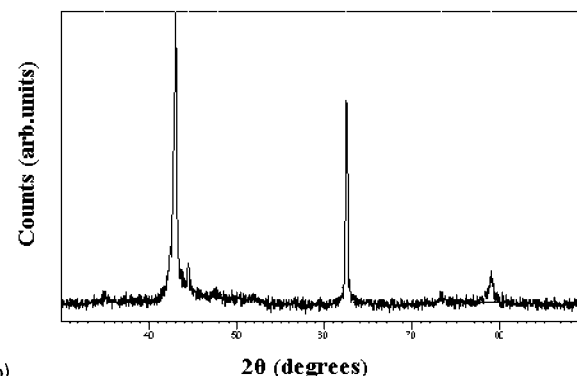
a 0·5 A dm^{-2}; *b* 1·5 A dm^{-2}
1 X-ray diffraction patterns observed for Zn–Ni pulse plated at current densities

value. Then the electrode potential was fixed as the open circuit potential. To the open circuit potential (OCP), the steady state polarisation was carried out from ±200 mV to the OCP at a scan rate of 1 mV s^{-1}. E_{corr} and i_{corr} values were obtained from the E v. log$i$ curves by the Tafel extrapolation method.

Results and discussion

Structural analysis

Figure 1 shows the typical XRD patterns of Zn–Ni coatings of ∼20 μm thickness produced by pulse plating on low carbon steel substrate at current density 0·5 and 1·5 A dm^{-2} respectively. The patterns show the polycrystalline nature of these coatings. The interplanar distance d, Miller indices hkl, intensity ratio I/I_o and the lattice parameter obtained from the XRD pattern of these coatings are presented in Table 3. The preferential orientation is along (411) for the coatings prepared with different current densities. Better crystallinity with a greater number of peaks was observed for the coatings

Table 2 Pulse plating parameters

	Pulse on–off time, ms							
	10		25		50		100	
	Time							
Duty cycle, %	On	Off	On	Off	On	Off	On	Off
10	10–90		4–36		2–18		1–9	
20	20–80		8–32		4–16		2–8	
30	40–60		16–24		8–12		4–6	
40	80–20		32–8		16–4		8–2	
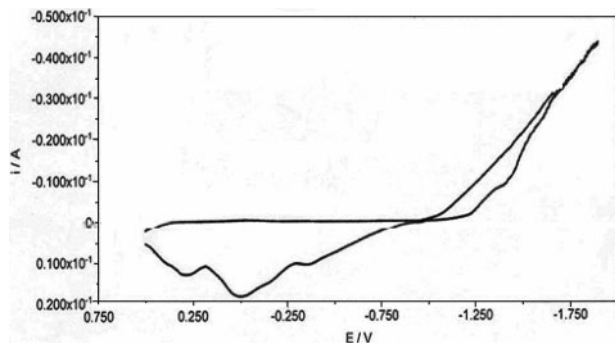
2 Cyclic voltammogram of Zn–Ni electrodeposited on glassy carbon: temperature=328 K, CD=1·5 A dm^{-2}, time=30 min

prepared under higher current density as shown in Fig. 1*b*. The phases of the deposits depend on the nickel content in the electrodeposited alloy. The deposit obtained consisted of a mixture of two phases δ-Ni_3Zn_{22} and δ-Ni_5Zn_{21} corresponding to the first two anodic peaks which appear in the cyclic voltammogram (Fig. 2), obtained on a glassy carbon electrode of 0·2 cm diameter that formed the working electrode of a three electrode cell assembly, with platinum as the auxiliary and saturated calomel as the reference electrodes.

Microstructure analysis

Scanning electron microscopy analysis

Figure 3 shows the SEM images of the pulse plated Zn–Ni alloy coatings, at current densities 0·5 and 1·5 A dm^{-2} respectively. The nucleation starts around scattered centres and deposits have nearly spherical

features. The surface showed a spherical nodular structure and the grains are very coarse. The average grain size was determined by Cottrell's method[22]

$$GS = 1 \cdot 5 l/mn \tag{5}$$

where l is the line drawn on the SEM picture, n is the number of grains on the line and m is the magnification.

The average grain sizes of the Zn–Ni alloy film deposited at 0·5 and 1·5 A dm^{-2} are 2·5 and 6 μm respectively.

The comparison of micrographs reveals a decrease in the grain size with increasing current density. The signature of decrease in grain size was identifiable from XRD line width measurements. This may be because at higher current density, the deposition rate is high and hence the adatoms get largely immobilised and are incorporated in the film with little surface migration, thereby limiting the grain size.

The coated samples were examined with AFM. The advantage of AFM is its capacity to probe minute details related to the individual grains and intergrain regions as well in three dimensional form. The representative topography of the pulse plated Zn–Ni alloy coatings at current density of 1·5 A dm^{-2} for a scanned area of 5×5 μm was examined. The image revealed a non-uniform globular structure, which was densely packed. Roughness analysis of the deposit was carried out and the value of the mean roughness Ra was calculated as the deviations in height from the profile mean value.[23]

$$Ra = \frac{1}{N} \sum_{I=1}^{N} |Z_i - Z| \tag{6}$$
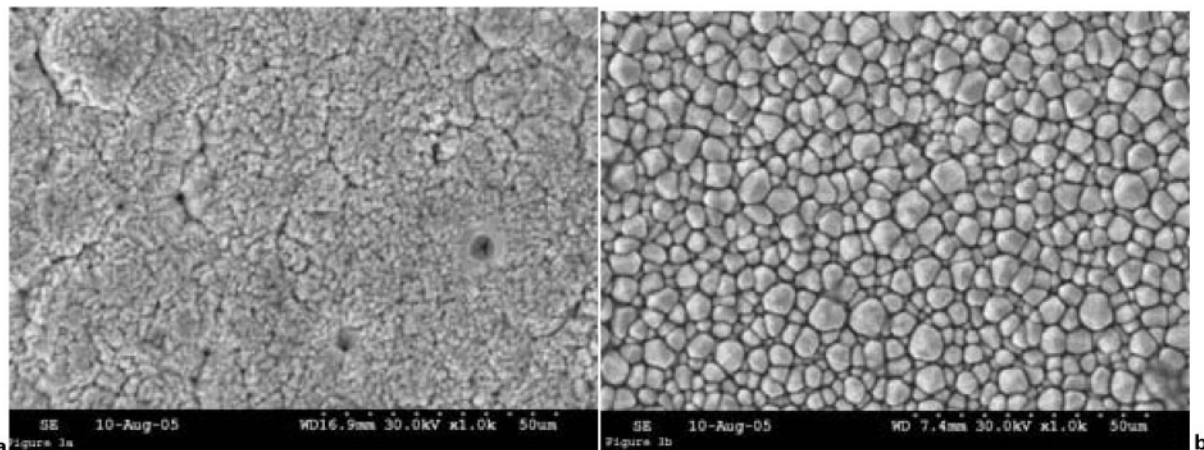
a 0·5 A dm^{-2}; *b* 1·5 A dm^{-2}
3 Photographs (SEM) of Zn–Ni pulse plated at current densities: at room temperature, for 30 min

Table 3 Data obtained from XRD analysis of pulse plated Zn–Ni deposits

Deposit	'*d*' spacing		Phase	*hkl*	Lattice parameters
	Observed	Standard			
Zn–Ni, pulse plated, 0·5 A dm^{-2}	2·11191	2·1000	Tetragonal	(330)	δ-Ni_3Zn_{22}: a=8·922, c=9·253
	1·49151	1·490	Cubic/bcc	(600)	Ni_5Zn_{21}: a=8·920
	1·21763	1·215		(552)	Ni_5Zn_{21}: a=8·920
Zn–Ni, pulse plated, 1·5 A dm^{-2}	2·09306	2·1000	Tetragonal	(330)	δ-Ni_3Zn_{22}: a=8·922, c=9·253
	2·03480	2·0000		(214)	–
	1·89989	1·908	Cubic/bcc	(332)	Ni_5Zn_{21}: a=8·920
	1·28982	1·291		(444)	–
	1·21136	1·215		(552)	–
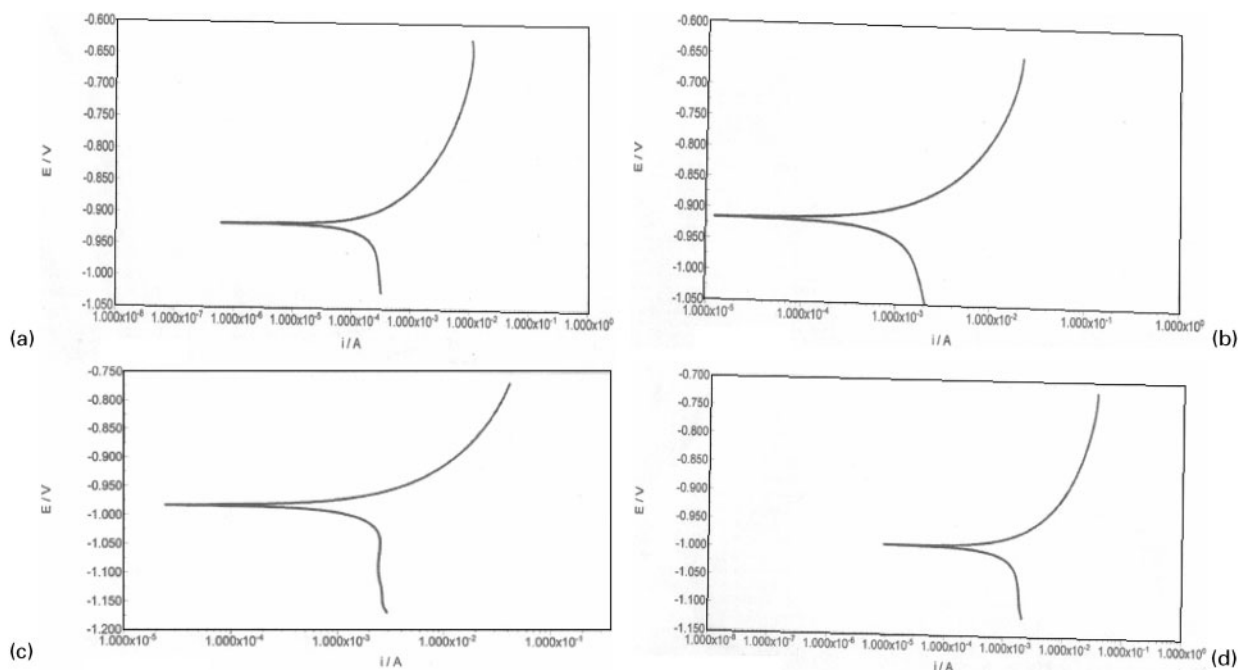
a at room temperature, on–off time 2–18; *b* at room temperature, on–off time 8–2; *c* at 40°C, on–off time 2–18; *d* at 40°C, on–off time 8–2

4 Potentiodynamic polarisation curve for pulse plated Zn–Ni electrodeposits obtained at current density 1·5 A dm^{-2} in 3·5%NaCl

where Z is defined as the sum of all height values divided by the number of data points N in the profile. The roughness value estimated from the image was 29 nm. The deposit is non-homogeneous as the roughness value is high.

Table 4 presents data on microhardness of the Zn–Ni deposits. As is seen from the table, pulse plated samples have on average double the microhardness of dc plated samples, probably due to the increased nickel content in the deposit. Table 5 gives the roughness values of the Zn–Ni deposits. The roughness values of pulse plated samples are decreased by on average less than three times, contributing to a smoother surface. Table 6 gives the composition of the coatings obtained from X-ray fluorescence studies. Pulse plated samples have higher nickel contents than dc plated ones, which contributes to greater corrosion resistance.

Corrosion behaviour

The principal aim of potentiodynamic polarisation studies carried out was to study surface degradation resulting from electrochemical processes and this necessitated an analysis of the surface deposit left after the electrochemical reactions. Potentiodynamic polarisation curves obtained for the pulse plated zinc–nickel electrodeposits on mild steel substrates, at current density 1·5 A dm^{-2}, for 30 min and at on–off times 2–18 and 8–2, are shown in Fig. 4.

The electrodeposition of zinc–nickel alloy is classified as anomalous.[24] The deposition of the more noble metal, nickel, is suppressed by the preferential deposition of zinc. For the anomalous codeposition, a concept based on the work function has been suggested.[25,26] If the work function of the alloy has been between that of the parent metals, then continuous underpotential of the nickel is possible. As the electrodeposition is carried out over a prolonged period, it may cause the pH to change near the surface. This would result in the precipitation of $Zn(OH)_2$. The anomalous codeposition of zinc–nickel alloy may be due to an increase in the surface pH causing the formation of $Zn(OH)_2$ which may suppress nickel discharge, or zinc deposition may be controlled by mass transport and nickel deposition by kinetics, or the rate of charge transfer of $ZnOH^+$ and $NiOH^+$ species may be responsible, or the monolayer coverage of nickel

Table 5 Roughness data of deposits

Electrodeposit	Roughness, μm
Zn–Ni, dc plated, 1·5 A dm^{-2}	0·62
Zn–Ni, pulse plating 0·5 A dm^{-2}	0·24
Zn–Ni, pulse plating 1·0 A dm^{-2}	0·10
Zn–Ni, pulse plating 1·5 A dm^{-2}	0·14
Zn–Ni, pulse plating 2·0 A dm^{-2}	0·13

Table 6 XRF data of deposits

Electrodeposit	Mass, %	
	Zinc	Nickel
Zn–Ni dc plated, 1·5 A dm^{-2}	82·02	17·98
Zn–Ni pulse plating, 0·5 A dm^{-2}	83·49	16·51
Zn–Ni pulse plating, 1·0 A dm^{-2}	80·64	19·36
Zn–Ni pulse plating, 1·5 A dm^{-2}	76·95	23·05
Zn–Ni pulse plating, 2·0 A dm^{-2}	76·05	23·95

Table 4 Microhardness data of Zn–Ni deposits

Electrodeposit	H_V
Zn–Ni, dc plated, 1·5 A dm^{-2}	119·1
Zn–Ni, pulse plated, 0·5 A dm^{-2}	390·8
Zn–Ni, pulse plated, 1·0 A dm^{-2}	362·6
Zn–Ni, pulse plated, 1·5 A dm^{-2}	350·4
Zn–Ni, pulse plated, 2·0 A dm^{-2}	186·5

Table 7 Parameters derived from potentiodynamic polarisation method in 3·5%NaCl

Electrodeposit	On–off time, s	E_{corr}, V	Tafel slope, V/decade		10^4 corrosion current density, A cm^{-2}	
			ba	bc	Anodic	Cathodic
Zn–Ni, dc plated, RT	–	−0·983	−0·096	−0·098	−0·968	1·063
Zn–Ni, pulse plated, RT	2–18	−0·918	−0·056	−0·076	−0·938	1·111
Zn–Ni, pulse plated, RT	8–2	−0·916	−0·056	−0·058	−0·921	3·175
Zn–Ni, pulse plated, 40°C	2–18	−0·984	−0·042	−0·044	−0·987	5·849
Zn–Ni, pulse plated, 40°C	8–2	−0·993	−0·042	−0·086	−1·007	6·433

may be followed by water molecule chemisorption with the formation of NiOH$^+$ (ads). As a result of the competition of zinc and nickel ions to occupy active sites, the preferential deposition of Zn and suppression of nickel take place. As the electrodeposition was carried out for a prolonged period, an increase in surface OH$^-$ ion concentration caused the precipitation of Zn(OH)$_2$. The suppression of Zn(OH)$_2$ growth favoured the discharge of nickel ions. Hence, an increased amount of nickel was seen on the surface of pulse plated alloy deposits. The formation of δZn$_3$Ni$_{22}$ was favoured as the Zn(OH)$_2$ precipitation was hindered.

The Stern–Geary equation[27] shows that

$R_{ct} =$ charge transfer resistance

$$= \frac{b_a b_c}{2·303 (b_a + BC)i_{corr}} \quad (7)$$

where i_{corr} is the corrosion current density.

Table 7 gives the parameters derived from potentiodynamic polarisation method in 3·5%NaCl solution for Zn–Ni deposits obtained by dc and pulse plating, at a current density of 1·5 A dm^{-2}, for 30 min.

Conclusions

Pulse plating from a zinc–nickel sulphamate bath at pH 3–4 produced semibright, smooth and uniform grey Zn–Ni deposits by enhancing the surface coverage as revealed by SEM and XRD analyses and also confirmed by roughness and hardness testing. The uniform nature of the coatings was observed from profilometric roughness measurement and microstructure analysis.

Pulse plated zinc–nickel alloy has an increased nickel content in the deposit, which increases the corrosion resistance. The positive shift in E_{corr} observed for the Zn–Ni plated samples from the E_{corr} values of the Zn–Ni deposited by the pulse technique is indicative of increased corrosion resistance. The observed decrease in I_{corr} for these samples confirms their improved corrosion resistant behaviour. This is due to the absence of pores in the deposits.

References

1. S. A. Watson: in 'Nickel Development Institute review', series no. 13001; 1998, Toronto, Nickel Development Institute.
2. F. C. Potter, A. M. Stoneman and R. G. Thilthorp: *Trans. IMF*, Apr. 1987, 115.
3. D. E. Hall: *Plat. Surf. Finish.*, 1983, **70**, 59.
4. N. Miura: *Trans. ISIJ*, 1983, **23**, 913.
5. B. Meuthen: *Plat. Surf. Finish.*, 1985, **74**, 40.
6. J. Divisek, P. Malinowski, J. Mergel and H. Schmitz: *Int. J. Hydr. Energy*, 1988, **13**, 141.
7. M. J. de Giz, S. A. Machodo, L. A. Avaco and E. R. Gonzalez: *J. Appl. Electrochem.*, 1992, **22**, 973.
8. J. Giridhar and W. J. Wanm Ooij: *Surf. Coat. Technol.*, 1992, **53**, 35.
9. R. G. Baker and C. A. Holden: *Plat. Surf. Finish.*, 1965, **72**, 54.
10. G. F. Hsu: *Plat. Surf. Finish.*, 1984, **781**, 52.
11. G. N. K. Ramesh Babu, G. Devaraj, J. Ayyappa Raju and R. Subramanian: Proc. Sympos. on 'Industrial metal finishing', Karaikudi, India, July 1985, Central Electrochemical Research Institute, 231–235.
12. B. Arsenault, B. Champagne, P. Lambert and S. Dallaire: IGM88 Tc-301-668-G, 1988.
13. R. Ramanauskas, L. Gudaviciute, O. Scit, D. Bucinskiene and R. Juskenas: *Trans. IMF*, 2008, **86**, (2), 103.
14. R. Ramanauskas, L. Gudaviciute, R. Juskenas and O. Scit: *Electrochim. Acta*, 2007, **53**, 1801.
15. J. L. Ortiz-Aparicio, Y. Meas, G. Trejo, R. Ortega, T. W. Chapan, E. Chainet and P. Ozil: *Electrochim. Acta*, 2007, **52**, 4742.
16. R. Ramanauskas, L. Gudaviciute, A. Kalinicenko and R. Juskenas: *J. Solid State Electrochem.*, 2005, **9**, 900.
17. J.-Y. Fei and G. D. Wilcox: *Electrochim. Acta*, 2005, **50**, 2693.
18. C. J. Chen and C. C. Wan: *J. Electrochem. Soc.*, 1989, **136**, 2050.
19. J. C. Puippe and F. H. Leaman (eds.): 'Theory and practice of pulse plating'; 1986, Orlando, FL, AESF Society.
20. I. Nanov, I. Gadshov and K. Pangarov: *Galvanotechnik*, 1984, **75**, 1107.
21. V. Ravindran and V. S. Muralidharan: *J. Sci. Ind. Res.*, 2003, **62**, 718.
22. V. D. Das and L. Damodare: *Solid State Commun.*, 1997, **103**, 173.
23. M. Koch and U. Eberbach: *Surf. Eng.*, 1997, **13**, (2), 157.
24. J. R. Smith, S. Breakspear and S. A. Campbell: *Trans. IMF*, 2003, **81**, (3), B55.
25. M. Mathias and T. Chapman: *J. Electrochem. Soc.*, 1987, **134**, 1408.
26. M. Mathias and T. Chapman: *J. Electrochem. Soc.*, 1990, **137**, 102.
27. M. Stern and A. N. Geary: *J. Electrochem. Soc.*, 1957, **104**, 56.